J Nanostruct 11(4): 638-646, Autumn 2021

RESEARCH PAPER

Enhancing AsH_3 Gas Adsorption Potentials of Graphitic Carbon Nitride by Codoping Cr/P, Mo/P, and W/P Atoms: A DFT Investigation

Ali Nematollahzadeh [1], Hadi Basharnavaz [2], Aziz Habibi-Yangjeh [2], and Seyed Hossein Kamali [2]*

[1] *Department of Chemical Engineering, University of Mohaghegh Ardabili, Ardabil, Iran*

[2] *Department of Chemistry, Faculty of Science, University of Mohaghegh Ardabili, Ardabil, Iran*

ARTICLE INFO

Article History:
Received 11 June 2021
Accepted 18 September 2021
Published 01 October 2021

Keywords:
AsH_3 adsorption
Density functional theory simulations
Graphitic carbon nitride
Transition metal/P–codoped g-C_3N_4

ABSTRACT

The adsorption mode of arsine (AsH_3) molecules on the P–doped, Cr–, Mo–, W–embedded, and also Cr/P–, Mo/P–, and W/P–codoped graphitic carbon nitride (g-C_3N_4) compounds were investigated upon density functional theory (DFT) computations. The calculated adsorption energy of AsH_3 gas on the aforementioned systems were -0.508, -2.413, -2.642, -3.094, -2.432, -2.702, and -3.105 eV, respectively. These results displayed that the sensitivity of g-C_3N_4 system for the adsorption of AsH_3 gas can be significantly improved by introducing an appropriate transition metal (TM) dopant. Therefore, the TM/P–modified g-C_3N_4 systems were found more suitable for adsorption and detection of AsH_3 gas than the pure g-C_3N_4 system. Furthermore, the band structure results illustrated that with codoping of Cr/P, Mo/P, and W/P atoms on the g-C_3N_4 and then adsorption of AsH_3 molecules, the electrical conductivity of systems remarkably reduces due to the created new impurity energy levels close to the Fermi level. The results of the relaxed structures revealed that with adsorption of AsH_3 on the g-C_3N_4 and the modified g-C_3N_4 with TM/P atoms, the initial structure of g-C_3N_4 system automatically chances from planar to wrinkles structure. In addition, the results of charge transfer analysis showed that the electron density accumulation region is located on the orbitals of AsH_3 molecules, resulting from the electron transfer from TM–modified g-C_3N_4 systems to AsH_3 gas. Overall, it can be inferred that the W/P–codoped g-C_3N_4 with the highest adsorption energy of -3.105 eV is more suitable than those of Cr/P– and Mo/P–codoped g-C_3N_4 systems for detecting and removing of AsH_3 molecules from the environment.

How to cite this article
Nematollahzadeh A., Basharnavaz H., Habibi-Yangjeh A., Kamali S.H. Enhancing AsH_3 Gas Adsorption Potentials of Graphitic Carbon Nitride by Codoping Cr/P, Mo/P, and W/P Atoms: A DFT Investigation. J Nanostruct, 2021; 11(4): 638-646. DOI: 10.22052/JNS.2021.04.001

INTRODUCTION

Arsine (AsH_3) is a dangerous material with high concern about skin, lung, and bladder owing to its extreme volatility and toxicity [1-3]. AsH_3 is slightly soluble in water, colorless, and with mild garlic-like odor in the gas form [4, 5]. It can trigger serious health problems even if a low amount of arsine gas was ingested into the human body causing long-term chronic diseases such as arsenicosis and acute fatal intoxication [6-8]. Removal of AsH_3 from a gas phase is an important matter, especially in industry. Hence, finding an efficient adsorbent for removing arsine gas from the atmosphere is essential. In this regard, several compounds

* *Corresponding Author Email: nematollahzadeha@uma.ac.ir*

have been recognized for AsH_3 gas detection and removal. Among various compounds, graphitic carbon nitride (g-C_3N_4) has the highest selectivity for AsH_3 molecules amongst the other adsorbents due to its excellent characteristics such as suitable band gap energy (E_g=2.7 eV), low cost, and excellent physicochemical stability [9-11]. These novel features make g-C_3N_4 a promising candidate for different fields, such as H_2 production from H_2O splitting, gas storage, reduction of CO_2, and toxic gas sensors [12-14]. Additionally, a vast number of attempts have been made in recent years by several strategies such as embedding, decorating, and doping different elements to improvise the AsH_3 gas sensing and removing via g-C_3N_4-based compounds [15-18].

The effect of B and P atoms codoping on optical and electronic characteristics of g-C_3N_4 were demonstrated by Moshfegh and co-workers [19] using *ab-initio* simulations. They found that the incorporation of both P and B into the structure of g-C_3N_4 decreases the E_g for pristine g-C_3N_4 from 3.1 eV to 1.9 eV. Vovusha *et al.* [20] reported the adsorption behavior of CO_2 on the Cr–, Co–, Ni–, Mn–, Sc–, Fe– Zn–, and Cu–doped g-C_3N_4 systems using VASP code. The results illustrated that these modified g-C_3N_4 compounds could be used for carbon dioxide gas storage. In another work, the adsorption manner of SO_2 molecules over the Ir/P–, Rh/P–, and Co/P–codoped g-C_3N_4 compounds were studied by DFT calculations [21]. The results indicated that the Ir/P–codoped g-C_3N_4 with the highest adsorption energy (E_{ads}) of -3.52 eV can be successfully utilized for the detecting and removing of sulfur dioxide from the atmosphere. In another report, Basharnavaz and co-workers [22] reported the adsorption manner of NO over the pristine g-C_3N_4, Fe–, Os–, and Ru–embedded g-C_3N_4 using DFT computations. They found that among these transition metal (TM)–modified g-C_3N_4 systems, the Os–embedded with E_{ads} of -3.14 eV has a promising candidate for detecting and removing of NO gas. Furthermore, the adsorption of CO gas on the g-C_3N_4, Pd–, Pt–, and Ni–embedded g-C_3N_4 were reported using *ab-initio* computations [23]. The results revealed that the g-C_3N_4, Pd–, and Ni–embedded g-C_3N_4 are non-magnetic, while Pt–embedded g-C_3N_4 system induces a magnetic moment of 1.35 μ_B. In addition, they found that Pt–embedded g-C_3N_4 with the highest E_{ads} of -2.77 eV is an excellent candidate for detecting and removing carbon monoxide gas from the environment. Furthermore, the adsorption behavior of NO_2 over the g-C_3N_4 and Rh–, Ir–, and Co–embedded g-C_3N_4 were investigated in order to explore the removing abilities of TM–modified g-C_3N_4 as NO_2 sensor [24]. The results displayed that the interaction between NO_2 gas and Ir–embedded system (with the highest E_{ads}=-4.47 eV) is higher than those of the other TM–modified g-C_3N_4 compounds. In another work, the adsorption behavior of several toxic gases such as H_2S, NO, and SO_2 on the pure and Mo–decorated g-C_3N_4 systems were reported using *ab-initio* computations [25]. The results demonstrated that the interaction energy between these toxic gas and Mo–decorated g-C_3N_4 is stronger than that of the pure system. Herein, a summary about the adsorption of arsine gas on the various adsorbents along with E_{ads} are summarized in Table 1 [26-32]. From this Table, it can be found that the adsorption energy of AsH_3 gas molecules on the Fe–doped single-walled carbon nanotube with the highest adsorption energy of -2.48 eV is higher than those of the other adsorbents [29].

In this research, we investigated the adsorption manner of AsH_3 gas on the P–doped, Cr–, Mo–, W–embedded, and also Cr/P–, Mo/P–, and W/P–codoped g-C_3N_4 systems using DFT computations in order to introduce suitable systems for application in sensing and removing of AsH_3 gas. To the best of the authors' knowledge there is no report on these TM/P–modified g-C_3N_4 systems as AsH_3 sensor, though numerous literature reports have focused on the adsorption of AsH_3 gas on several adsorbents.

COMPUTATIONAL METHODS

In this study, all of the relaxed computations were performed with the Quantum Espresso (QE) package based on DFT computations. The generalized gradient approximation (GGA) with the Perdew–Burke–Ernzerhof (PBE) exchange–correlation was utilized to explain the correlation and exchange effects. It should be noted that the used DFT exchange-correlation functional tends to underestimate adsorption energy, therefore the DFT computations coupled with a van der Waals (vdW)-inclusive corrections of Grimme (DFT-D) are carried out to improve the computations. A Monkhorst-Pack (MP) grid of 1×1×8 was carried out to perform Brillouin-zone (BZ) integrations. The kinetic energy cut-off equal to 90 Ry was chosen and a vacuum space of 18 Å was inserted

Table 1. Comparison between previous studies and this work about AsH_3 adsorption onto different adsorbents.

Adsorbent	E_{ads} (eV)	Software	Phase	Year	Reference
P-doped g-C_3N_4[1]	-0.50	Quantum Espresso	Solid state	2019	This work
Cr-embedded g-C_3N_4	-2.41				
Cr/P-co doped g-C_3N_4	-2.43				
Mo-embedded g-C_3N_4	-2.64				
Mo/P-co doped g-C_3N_4	-2.70				
W-embedded g-C_3N_4	-3.09				
W/P-co doped g-C_3N_4	-3.10				
Pristine graphene	-0.04	Dmol[3]	Solid state	2019	[26]
Ti-doped graphene	-0.95				
Mn-doped graphene	-1.20				
Fe-doped graphene	-1.51				
Co-doped graphene	-1.27				
Ni-doped graphene	-1.72				
Cu-doped graphene	-1.38				
Ag-doped graphene	-1.77				
V_2O_5(001)	-0.069	VASP	Solid state	2019	[27]
S-vacancy MoS_2 monolayer	-0.417	ATK	Solid state	2019	[28]
Mo-vacancy MoS_2 monolayer	-0.563				
Pristine CNT[2]	-0.011	Gaussian g09	Gas phase	2018	[29]
Fe-doped CNT	-2.48				
Pd-doped CNT	-0.779	Dmol[3]	Solid state	2018	[30]
Pd-doped graphene	-1.00	Dmol[3]	Solid state	2016	[31]
Pristine CNT	-0.014				
Sc-doped CNT	-0.490	DFT	Gas phase	2016	[32]
Ti-doped CNT	-0.627				
V-doped CNT	-0.898				
Cr-doped CNT	-0.835				

[1] Graphitic carbon nitride
[2] Carbon nanotube

along the z-direction of g-C_3N_4 surface to avoid the interaction between the periodic layers.

The E_{ads} of AsH_3 gas over the P–doped and TM/P–modified g-C_3N_4 systems can be calculated by expression as given below [33]:

$$E_{ads} = E_{g-C_3N_4-AsH_3} - E_{AsH_3} - E_{g-C_3N_4} \quad (1)$$

where $E_{g-C_3N_4-AsH_3}$, E_{AsH_3}, and $E_{g-C_3N_4}$ are the total energy of AsH_3 adsorbed over the g-C_3N_4 systems, free AsH_3 gas, and g-C_3N_4, respectively. A more negative value of E_{ads} suggests that the adsorption behavior of AsH_3 gas molecule over the g-C_3N_4 surface is energetically more favorable.

Additionally, one of an important parameter for the adsorption process of a toxic gas sensing device is the recovery time (τ), thus the τ of AsH_3 gas from P–doped and Cr/P–, Mo/P–, and W/P–modified g-C_3N_4 systems can be predicted from the following equation [34]:

$$\tau = \vartheta_0^{-1} \exp\left(\frac{-E_{ads}}{kT}\right) \quad (2)$$

where ϑ_0, k, E_{ads}, and T indicates attempted frequency (ϑ_0=10^{12} s^{-1}), Boltzmann's constant (k = 8.62×10^{-5} eV K^{-1}), adsorption energy and temperature, respectively. The computed recovery time for the P–doped, Cr–, Mo–, W–embedded, Cr/P–, Mo/P–, and W/P–codoped g-C_3N_4 systems are seen to be 3.90×10^{-4}, 6.42×10^{28}, 4.79×10^{32}, 2.11×10^{40}, 1.34×10^{29}, 4.96×10^{33} and 3.24×10^{40} s, respectively. According to this equation, the more negative value for the adsorption energy leads to the extended recovery time due to prolonged desorption of gas molecules from the surface of adsorbent. Thus, it is inferred that the strong interaction energy between AsH_3 gas and W/P–codoped g-C_3N_4 system with the highest E_{ads}=-3.105 eV revealed that the g-C_3N_4–based materials, gradually recover to its a stable initial state [35].

RESULTS AND DISCUSSION

In this article, a systematic theoretical investigation of AsH_3 gas adsorption by P–doped, Cr–, Mo–, and W–embedded, and also Cr/P–, Mo/P–, and W/P–codoped g-C_3N_4 compounds were

explored using DFT computations. The optimized structures for adsorption of AsH_3 molecules over the P–doped and TM/P–codoped g-C_3N_4 systems are shown in Fig. 1. The results of the literature review displayed that the adsorption energy of AsH_3 gas on different TM–modified adsorbents from As atom is stronger than that of H atom [29, 32]. Comparing optimized structures of P–doped and Cr/P–, Mo/P–, and W/P–codoped g-C_3N_4 systems in Fig. 1, it is clearly seen that there is a remarkable change in relaxed structures of these g-C_3N_4 before and after the adsorption of AsH_3 gas. On the other hand, with adsorption of AsH_3 gas molecules on the g-C_3N_4 system and also codoping of g-C_3N_4 with TM and P elements, the primary flat structures of pure g-C_3N_4 automatically changed to buckle structure [36, 37].

To further explore the effect of AsH_3 gas adsorbing on the electronic characteristics of g-C_3N_4 systems, the band structures plots for P–doped, Cr–, Mo–, W–embedded, and also Cr/P–, Mo/P–, and W/P–codoped g-C_3N_4 systems are demonstrated in Fig. 2 and also the corresponding data are listed in Table 2. It is worth noting that the Fermi energy level was set to zero energy scale (red dotted line). The results of band structures revealed that the E_g for

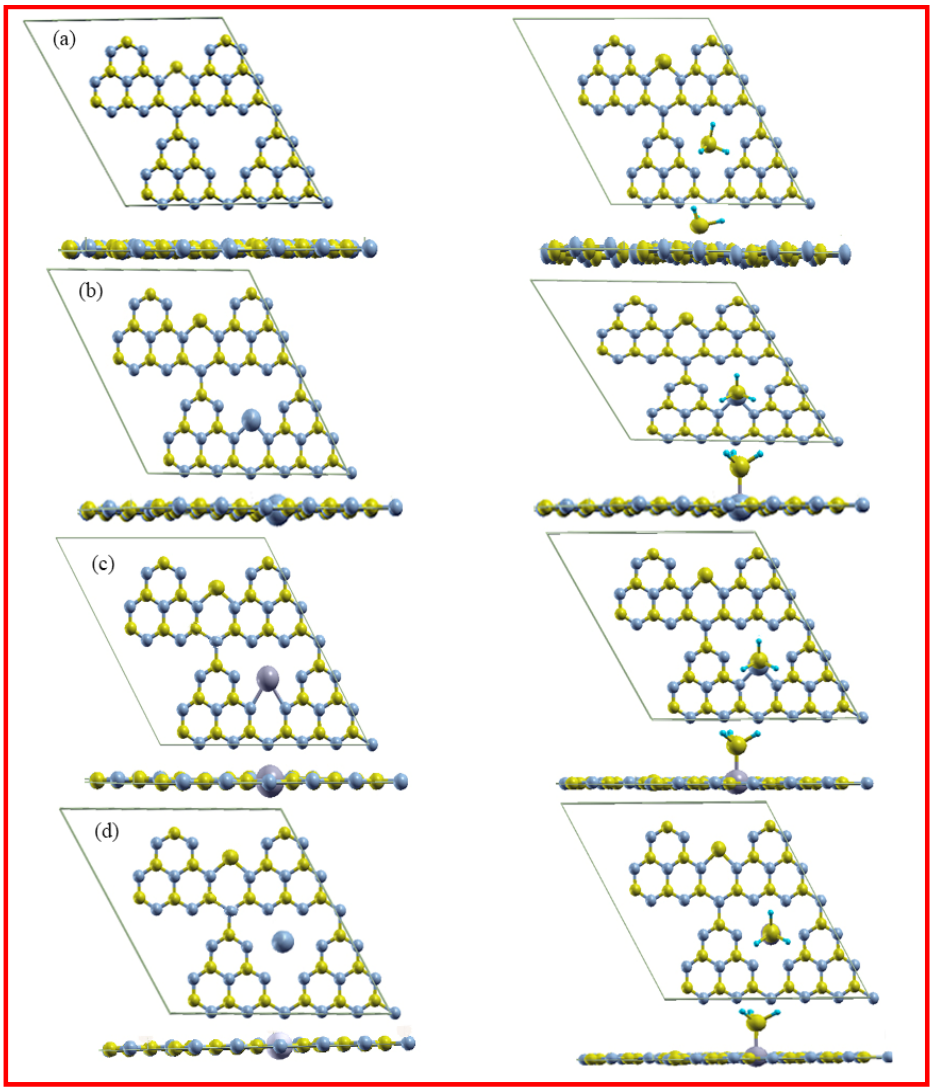

Fig. 1. The optimized structures for the P–doped and TM/P–codoped g-C_3N_4 systems before and after adsorption of AsH_3 gas: (a) P–doped, (b) Cr/P–, (c) Mo/P–, and (d) W/P–codoped g-C_3N_4. The carbon and nitrogen elements are displayed by yellow and blue spheres, respectively.

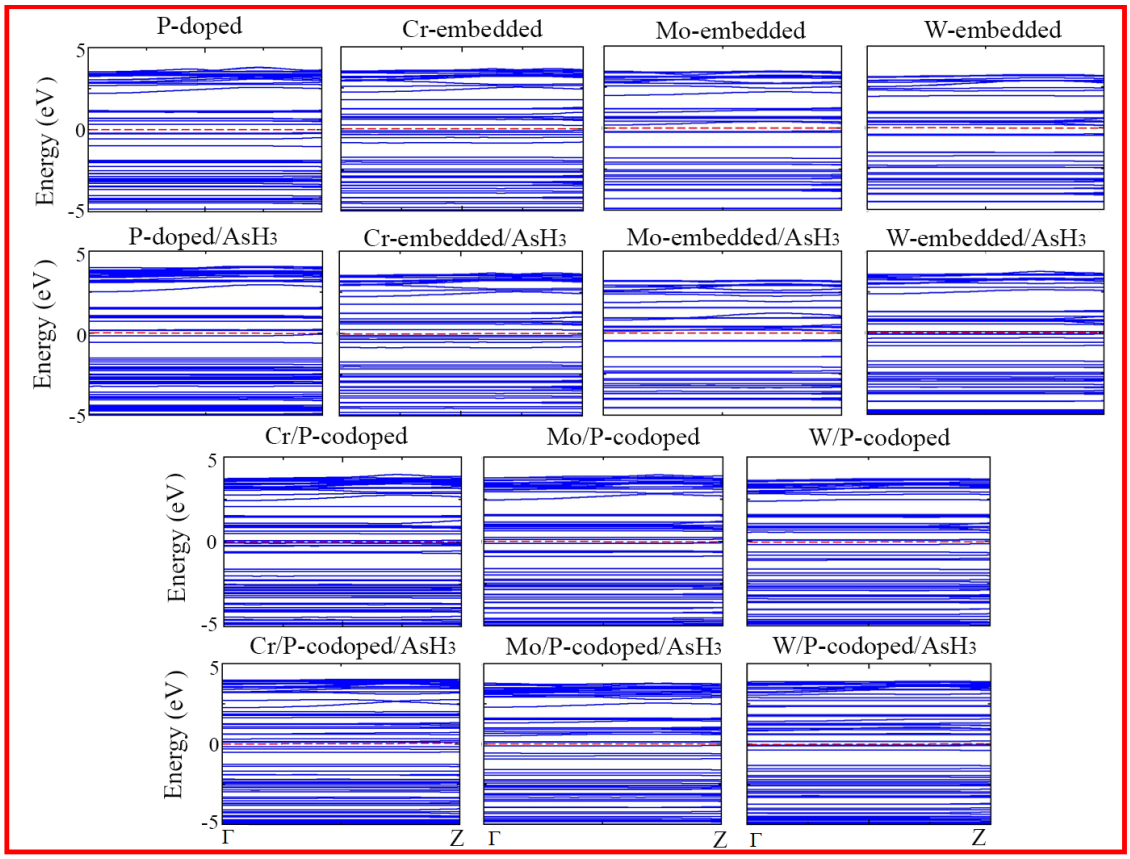

Fig. 2. Electronic band structures for the P–doped, Cr–, Mo–, W–embedded, and also Cr/P–, Mo/P–, and W/P–codoped g-C_3N_4 systems before and after adsorption of AsH_3 gas. The band structures are demonstrated along the ΓZ direction. The E_F levels are at zero eV and are represented by dotted lines.

Table 2. The structural parameters, adsorption energy (E_{ads}), band gap energy (E_g), total induced magnetic moment per unit cell (M_{tot}), Fermi energy level (E_F), and Lowdin charges for adsorption of AsH_3 gas molecules on the P–doped, Cr–, Mo–, W–embedded, and also Cr/P–, Mo/P–, and W/P–codoped g-C_3N_4 systems.

	Property	P-doped	Cr-embedded	Mo-embedded	W-embedded	Cr/P-codoped	Mo/P-codoped	W/P-codoped	P-doped/AsH_3	Cr-embedded/AsH_3	Mo-embedded/AsH_3	W-embedded/AsH_3	Cr/P-codoped/AsH_3	Mo/P-codoped/AsH_3	W/P-codoped/AsH_3
	E_g (eV)	0.45	0.30	0.29	0.28	0.15	0.14	0.13	0.40	0.28	0.26	0.15	0.10	0.08	0.06
	E_F (eV)	-0.36	-0.33	-0.23	-0.16	-0.16	-0.15	-0.14	-0.19	-0.22	-0.18	-0.15	-0.20	-0.14	-0.13
	E_{ads} (eV)	-	-	-	-	-	-	-	-0.508	-2.413	-2.642	-3.094	-2.432	-2.702	-3.105
	M_{tot} (μ_B)	0.00	0.25	0.31	0.44	0.20	0.29	0.39	0.00	0.21	0.14	0.00	0.18	0.10	0.00
Bond Length (Å)	d(As-H)	-	-	-	-	-	-	-	1.525	1.530	1.537	1.538	1.535	1.539	1.541
Bond Length (Å)	embedded–As	-	-	-	-	-	-	-	-	2.390	2.430	2.386	2.387	2.423	2.382
Bond Length (Å)	Cr–N_{edge}	-	1.896	-	-	1.891	-	-	-	1.917	-	-	1.912	-	-
Bond Length (Å)	Mo–N_{edge}	-	-	2.242	-	-	2.226	-	-	-	2.406	-	-	2.355	-
Bond Length (Å)	W–N_{edge}	-	-	-	2.413	-	-	2.354	-	-	-	2.440	-	-	2.434
Lowdin	H (AsH_3)	0.042	-	-	-	-	-	-	0.041	0.040	0.038	0.036	0.040	0.039	0.034
Lowdin	As (AsH_3)	-0.034	-	-	-	-	-	-	-0.096	-0.714	-0.881	-0.987	-0.797	-1.011	-1.091
Lowdin	N_{edge} (g-C_3N_4)	-0.339	-	-	-	-	-	-	-0.327	-0.269	-0.252	-0.240	-0.247	-0.237	-0.220

a pure g-C_3N_4 at the DFT calculation is smaller than the experimental value (E_g=2.70 eV), because the GGA functional underestimate the fundamental gap energy. It should be noted that the underestimation of E_g in the present investigation will not affect the ultimate conclusion because we aim to make the comparison for the adsorption performance and electrical characteristics of pure and TM/P–modified g-C_3N_4 systems with and without AsH_3 molecules. As shown in Fig. 2, with adsorption of AsH_3 molecules on the g-C_3N_4 and also codoping of Cr, Mo, W, and P atoms, the E_g of system (E_g=2.7 eV) is considerably decreased. Furthermore, it was found that the E_F of g-C_3N_4 system upshifts into the conduction band edge after the adsorption of AsH_3 molecules and also codoping of P and TM atoms, indicating the improvement of the conductivity of these modified g-C_3N_4 systems. Additionally, these results indicated that the AsH_3–adsorbed and TM/P–modified g-C_3N_4 systems have semi-metallic properties because valence band and conduction band energy levels have not crossed each other at near the Fermi energy. Thus, it is inferred that the electrical conductivity of g-C_3N_4 systems are considerably modulated by adsorption of AsH_3 and also codoping with Cr, Mo, W, and P atoms (see Table 2).

The total induced magnetic moment (M_{tot}) and geometrical parameters of AsH_3 gas adsorbed over the P–doped and Cr/P–, Mo/P–, and W/P–modified g-C_3N_4 systems such as As–H bond length (d_{As-H}), TM–N_{edge} bond length, and distance between As atoms of arsine molecules and these TM elements are listed in Table 2. As seen, the magnetic moment for W/P–codoped (M_{tot}=0.39 μ_B) is higher than those of the Cr/P– and Mo/P–modified g-C_3N_4 systems, because the weak interaction between N_{edge} and W atoms causes induced magnetic features in this system. Furthermore, it can be realized that with adsorption of AsH_3 molecules on the W/P–codoped g-C_3N_4, the M_{tot} reduces from 0.39 to 0.00 μ_B. This phenomenon attributed to strong overlapping between orbitals of W and As atoms. In addition, the bond lengths of As–H are 1.525 Å (P–doped), 1.535 Å (Cr/P-codoped), 1.539 Å (Mo/P-codoped), and 1.541 Å (W/P-codoped) having a considerable variation in comparison with the bond length of free AsH_3 gas (1.520 Å). From Table 2, it can be observed that the bond lengths of TM–N_{edge} significantly change after adsorption of AsH_3 molecules over the TM/P–modified g-C_3N_4 compounds. It should be noted that the elongation of d_{As-H} in AsH_3–adsorbed W/P–codoped g-C_3N_4 is higher than those of the other TM/P–codoped systems. This phenomenon is mostly ascribed to the large electron transfer from the W/P–codoped g-C_3N_4 to AsH_3 gas. The maximum value of E_{ads} for AsH_3 adsorbed on the W/P–codoped g-C_3N_4 with the smaller distance between W and AsH_3 molecules indicating strong chemisorption for AsH_3 on this system (see Table 2).

The Lowdin charges analysis before and after adsorption of AsH_3 molecules on the P–doped, TM–embedded, and TM/P–codoped g-C_3N_4 compounds are displayed in Table 2. The negative value of the electron transfer shows that the electron is transferred from TM–modified g-C_3N_4 to AsH_3 molecules. On the other hand, the AsH_3 acts as an electronic charge acceptor and these TM–modified g-C_3N_4 compounds behave as electronic charge donor [27, 28]. In addition, it was found that the charge transfer between orbitals of g-C_3N_4 and AsH_3 gas in W/P–codoped system is more than those of the other g-C_3N_4 systems. The results of Lowdin charge displayed that the interaction energy between W/P–codoped and AsH_3 molecules is higher than those of the other reported systems.

In order to further explain the electronic characteristics of the g-C_3N_4 systems, the partial density of states (PDOS) for the N_{edge} orbitals of the P–doped, Cr–, Mo–, W–embedded, Cr/P–, Mo/P–, and W/P–codoped g-C_3N_4 compounds before and after adsorption of AsH_3 molecules are demonstrated in Fig. 3. From this figure, we can see that with codoping of Cr, Mo, W, and P elements and also adsorption of AsH_3 molecules on the g-C_3N_4, electron density close to the Fermi energy state for N_{edge} elements in these g-C_3N_4 systems remarkably increase, which is caused owing to the strong overlapping between orbitals of the different elements in the g-C_3N_4 systems and AsH_3 gas. This shows that there is a considerable charge transfer between AsH_3 gas and modified g-C_3N_4. In addition, it can be inferred that the sharp peak close to E_F for the N_{edge} element in AsH_3–adsorbed W/P–codoped g-C_3N_4 is more than those of the Cr/P–, Mo/P– codoped compounds, which reveals a strong interaction energy between W element and AsH_3 gas. Based on these results, it can be stated that the strong orbital hybridization between Cr, Mo, and especially W atoms and AsH_3 gas enhances the gas adsorption ability of the g-C_3N_4 compounds to this toxic gas.

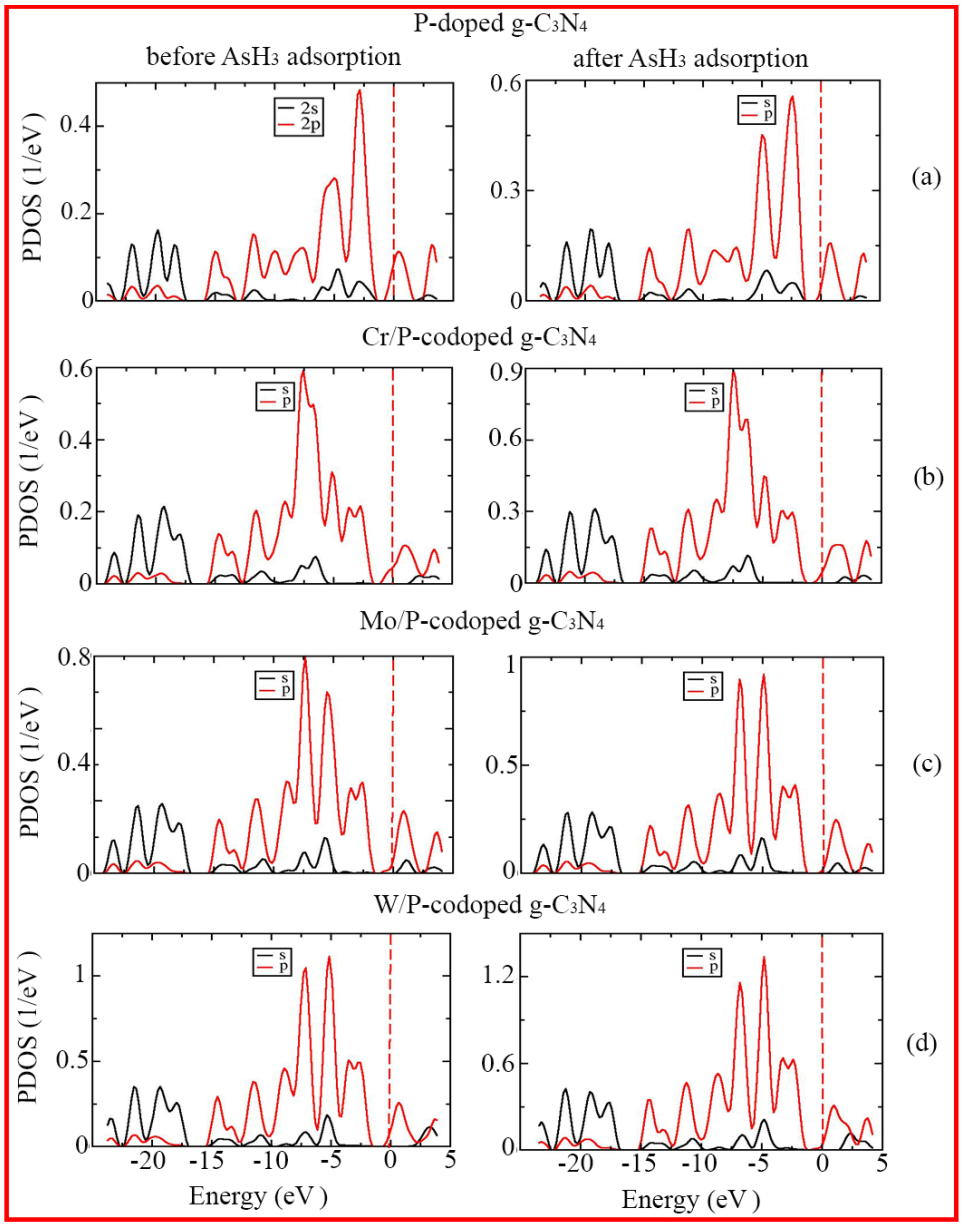

Fig. 3. PDOS for Nedge atoms in the P–doped and TM/P–codoped g-C_3N_4 systems: (a) P–doped, (b) Cr/P–, (c) Mo/P–, and (d) W/P–codoped g-C_3N_4. The E_F level was set at zero eV and are demonstrated by dotted lines

CONCLUSIONS

In this research, the adsorption manner of AsH_3 gas over the P–doped, Cr–, Mo–, W–embedded, Cr/P–, Mo/P–, and W/P–codoped g-C_3N_4 compounds were investigated by first–principles study. The results of adsorption energy displayed that the sensitivity of g-C_3N_4 system for the adsorption of AsH_3 gas can be considerably improved by introducing an appropriate transition metal (TM) dopant. Therefore, Cr/P–, Mo/P–, and W/P–codoped g-C_3N_4 are more appropriate for detection and adsorption of AsH_3 gas than that of the pristine g-C_3N_4. The results of electronic band structures revealed that with adsorption of AsH_3 molecules over the g-C_3N_4 systems and also codoping of TM and P atoms, the electrical conductivity of g-C_3N_4 remarkably reduces due to the induced new impurity energy levels close to Fermi energy level. Additionally, the results of relaxed structures indicated that with

adsorption of AsH_3 over the g-C_3N_4 systems and also modifying with these TM atoms, the initial structure of g-C_3N_4 system automatically chances from planar to wrinkles structure. Furthermore, the results of electron transfer indicated that the electron density accumulation region is located on the orbitals of AsH_3 gas molecules, resulting from the electron transfer from TM/P–codoped g-C_3N_4 systems to AsH_3 gas. Based on these results, it can be state that the W/P–codoped g-C_3N_4 with the highest adsorption energy of -3.105 eV is more suitable than those of the Cr/P– and Mo/P–codoped g-C_3N_4 systems for detecting and removing of AsH_3 from the atmosphere. On the other hand, the W/P–codoped g-C_3N_4 cannn be a good candidate for toxic gas sensors, providing an avenue to facilitate the design of highly active g-C_3N_4-based gas sensors.

CONFLICT OF INTEREST

The authors declare that there is no conflict of interests regarding the publication of this manuscript.

REFERENCES

1. Argos M, Parvez F, Chen Y, Hussain AI, Momotaj H, Howe GR, et al. Socioeconomic status and risk for arsenic-related skin lesions in Bangladesh. Am J Public Health. 2007;97(5):825-831.
2. Chen Y, Parvez F, Gamble M, Islam T, Ahmed A, Argos M, et al. Arsenic exposure at low-to-moderate levels and skin lesions, arsenic metabolism, neurological functions, and biomarkers for respiratory and cardiovascular diseases: review of recent findings from the Health Effects of Arsenic Longitudinal Study (HEALS) in Bangladesh. Toxicology and applied pharmacology. 2009;239(2):184-192.
3. Hughes MF, Beck BD, Chen Y, Lewis AS, Thomas DJ. Arsenic exposure and toxicology: a historical perspective. Toxicol Sci. 2011;123(2):305-332.
4. Furue R, Koveke EP, Sugimoto S, Shudo Y, Hayami S, Ohira S-I, et al. Arsine gas sensor based on gold-modified reduced graphene oxide. Sensors Actuators B: Chem. 2017;240:657-663.
5. Pakulska D, Czerczak S. Arsine. 2014.
6. Chung JS, Kalman DA, Moore LE, Kosnett MJ, Arroyo AP, Beeris M, et al. Family correlations of arsenic methylation patterns in children and parents exposed to high concentrations of arsenic in drinking water. Environ Health Perspect. 2002;110(7):729-733.
7. Mazumder DNG, Haque R, Ghosh N, De BK, Santra A, Chakraborti D, et al. Arsenic in drinking water and the prevalence of respiratory effects in West Bengal, India. Int J Epidemiol. 2000;29(6):1047-1052.
8. Meliker JR, Wahl RL, Cameron LL, Nriagu JO. Arsenic in drinking water and cerebrovascular disease, diabetes mellitus, and kidney disease in Michigan: a standardized mortality ratio analysis. Environ Health. 2007;6(1):4.
9. Zheng Y, Liu J, Liang J, Jaroniec M, Qiao SZ. Graphitic carbon nitride materials: controllable synthesis and applications in fuel cells and photocatalysis. Energy Environ Sci. 2012;5(5):6717-6731.
10. Algara-Siller G, Severin N, Chong SY, Bjorkman T, Palgrave RG, Laybourn A, et al. Triazine-based graphitic carbon nitride: a two-dimensional semiconductor. Angew Chem Int Ed Engl. 2014;53(29):7450-7455.
11. Abdullahi Y, Yoon TL, Halim MM, Roslan Hashim M, Lim T-L. Mechanical and electronic properties of graphitic carbon nitride sheet: First-principles calculations2016. 144-150 p.
12. Huang D, Yan X, Yan M, Zeng G, Zhou C, Wan J, et al. Graphitic Carbon Nitride-Based Heterojunction Photoactive Nanocomposites: Applications and Mechanism Insight. ACS Applied Materials & Interfaces. 2018;10(25):21035-21055.
13. Wu M, Wang Q, Sun Q, Jena P. Functionalized graphitic carbon nitride for efficient energy storage. The Journal of Physical Chemistry C. 2013;117(12):6055-6059.
14. Cao S, Yu J. g-C3N4-based photocatalysts for hydrogen generation. The journal of physical chemistry letters. 2014;5(12):2101-2107.
15. Zhu J, Diao T, Wang W, Xu X, Sun X, Carabineiro SAC, et al. Boron doped graphitic carbon nitride with acid-base duality for cycloaddition of carbon dioxide to epoxide under solvent-free condition. Applied Catalysis B: Environmental. 2017;219:92-100.
16. Ma DW, Wang Q, Yan X, Zhang X, He C, Zhou D, et al. 3d transition metal embedded C2N monolayers as promising single-atom catalysts: A first-principles study. Carbon. 2016;105:463-473.
17. Liu B, Ye L, Wang R, Yang J, Zhang Y, Guan R, et al. Phosphorus-Doped Graphitic Carbon Nitride Nanotubes with Amino-rich Surface for Efficient CO_2 Capture, Enhanced Photocatalytic Activity, and Product Selectivity. ACS Applied Materials & Interfaces. 2018;10(4):4001-4009.
18. Guo W, Zhang J, Li G, Xu C. Enhanced photocatalytic activity of P-type (K, Fe) co-doped g-C_3N_4 synthesized in self-generated NH3 atmosphere2018.
19. Yousefi M, Faraji M, Asgari R, Moshfegh AZ. Effect of boron and phosphorus codoping on the electronic and optical properties of graphitic carbon nitride monolayers: First-principle simulations. PhRvB. 2018;97(19):195428.
20. Hussain T, Vovusha H, Kaewmaraya T, Karton A, Amornkitbamrung V, Ahuja R. Graphitic carbon nitride nano sheets functionalized with selected transition metal dopants: an efficient way to store CO_2. Nanotechnology. 2018;29(41):415502.
21. Basharnavaz H, Habibi-Yangjeh A, Kamali SH. Adsorption performance of SO_2 gases over the transition metal/P–codoped graphitic carbon nitride: A DFT investigation. Materials Chemistry and Physics. 2019:122602.
22. Basharnavaz H, Habibi-Yangjeh A, Kamali SH. Fe, Ru, and Os–embedded graphitic carbon nitride as a promising candidate for NO gas sensor: A first-principles investigation. Materials Chemistry and Physics. 2019.
23. Basharnavaz H, Habibi-Yangjeh A, Kamali SH. A first-principles study on the interaction of CO molecules with VIII transition metals-embedded graphitic carbon nitride as an excellent candidate for CO sensor. Physics Letters A. 2019.
24. Basharnavaz H, Habibi-Yangjeh A, Kamali SH. A first-principle investigation of NO_2 adsorption behavior on Co, Rh, and Ir-embedded graphitic carbon nitride: Looking for highly sensitive gas sensor. Physics Letters A. 2019:126057.
25. Xu Y, Jiang S-X, Yin W-J, Sheng W, Wu L-X, Nie G-Z, et al.

Adsorption behaviors of HCN, SO_2, H_2S and NO molecules on graphitic carbon nitride with Mo atom decoration. Applied Surface Science. 2020;501:144199.
26. Li Y, Sun X, Zhou L, Ning P, Tang L. Density functional theory analysis of selective adsorption of AsH_3 on transition metal-doped graphene. J Mol Model. 2019;25(5):145.
27. Ranea VA, Quiña PLD, Yalet NM. General adsorption model for H_2S, H_2Se, H_2Te, NH_3, PH_3, AsH_3 and SbH_3 on the V_2O_5 (0 0 1) surface including the van der Waals interaction. Chemical Physics Letters. 2019;720:58-63.
28. Jasmine JM, Aadhityan A, Thiruvadigal DJ. A first-principles study of Cl_2, PH_3, AsH_3, BBr_3 and SF_4 gas adsorption on MoS2 monolayer with S and Mo vacancy. Applied Surface Science. 2019;489:841-848.
29. Arasteh J, Naseh M. DFT study of arsine (AsH_3) gas adsorption on pristine, Stone-Wales-defected, and Fe-doped single-walled carbon nanotubes. Struct Chem. 2019;30(1):97-105.
30. Shojaie F. Arsine adsorption on the surface of palladium-doped carbon nanotubes. Moroccan Journal of Chemistry. 2018;6(4):6-4 (2018) 2676-2688.
31. Kunaseth M, Mudchimo T, Namuangruk S, Kungwan N, Promarak V, Jungsuttiwong S. A DFT study of arsine adsorption on palladium doped graphene: effects of palladium cluster size. Applied Surface Science. 2016;367:552-558.
32. Buasaeng P, Rakrai W, Wanno B, Tabtimsai C. DFT investigation of NH_3, PH_3, and AsH_3 adsorptions on Sc-, Ti-, V-, and Cr-doped single-walled carbon nanotubes. Applied Surface Science. 2017;400:506-514.
33. Kumar S, Singh M, Sharma DK, Auluck S. Enhancing gas adsorption properties of borophene by embedding transition metals. Computational Condensed Matter. 2020;22:e00436.
34. Nagarajan V, Chandiramouli R. A novel approach for detection of NO_2 and SO_2 gas molecules using graphane nanosheet and nanotubes-A density functional application. Diamond and Related Materials. 2018;85:53-62.
35. Soltani A, Raz SG, Taghartapeh MR, Moradi AV, Mehrabian RZ. Ab initio study of the NO_2 and SO_2 adsorption on Al12N12 nano-cage sensitized with gallium and magnesium. Computational Materials Science. 2013;79:795-803.
36. Wu H-Z, Liu L-M, Zhao S-J. The effect of water on the structural, electronic and photocatalytic properties of graphitic carbon nitride. Physical Chemistry Chemical Physics. 2014;16(7):3299-3304.
37. Wu H-Z, Bandaru S, Liu J, Li L-L, Wang Z. Adsorption of H_2O, H_2, O_2, CO, NO, and CO_2 on graphene/g-C_3N_4 nanocomposite investigated by density functional theory. Applied Surface Science. 2018;430:125-136.